Measurement of Individual Cell Migration Parameters for Human Tissue Cells

Paul A. DiMilla and John A. Quinn
Dept. of Chemical Engineering, University of Pennsylvania, Philadelphia, PA 19104

Steven M. Albelda
Hospital of the University of Pennsylvania, Philadelphia, PA 19104

Douglas A. Lauffenburger
Depts. of Chemical Engineering and Cell & Structural Biology, University of Illinois at Urbana-Champaign, Urbana, IL 61801

We present an approach for determining in vitro the means and distributions of a set of phenomenological parameters, including cell speed and persistence time, which can be used to evaluate the effect of isotropic variations in the extracellular environment on the motility of human tissue cells. Using time-lapse videomicroscopy and semi-automated image analysis, we tracked the paths traveled by slow-moving, isolated human vascular smooth muscle cells over 48 hours on surfaces of petri dishes coated with 10 μg/mL of the adhesive extracellular matrix proteins type IV collagen, fibronectin or laminin. By applying a persistent random walk model to experimental data for mean-squared displacement as a function of time for these cells, we rigorously distinguished individual cells with different motile characteristics not obvious based on qualitative comparisons between the structures of individual cell paths. We also positively identified the presence of immotile cells. Based on the behavior of 34 to 77 cells on each substrate, we found mean cell speeds and persistence times on the order of 10 micron/h and 3 hours, respectively, on all three ECM substrates, while the fraction of motile cells varied from 65% on laminin to 78% on collagen. On all three surfaces experimental number distributions of speed and persistence time could be described by normal and exponential waiting time distributions, respectively. Our approach provides a framework for addressing questions concerning the mechanistic relationship between cellular and environmental properties and cell motility.

Introduction

Migration of mammalian tissue cells plays an important role in many physiological and pathological processes, including embryonic development, wound repair, angiogenesis, and the metastasis of tumor cells (Trinkaus, 1984). The motile behavior of human vascular smooth muscle cells (HSMCs), which form the underlying supporting tissue of large blood vessels, demonstrates the diverse range of consequences that can result from tissue cell motility. While HSMC movement is beneficial for restructuring the cardiovascular system during development and growth, HSMC migration in adults has been associated with the development of atherosclerotic plaques (Ross, 1986) and deleterious vascular remodeling after injury (Clyman et al., 1990).

Because of the fundamental importance of migration *in vivo*, cell movement often has been studied *in vitro*. Common techniques for investigating the motile behavior of tissue and white blood cells, including the Boyden chamber, wound, and phagokinetic track assays, assess the motility of either a cell population or individual cells (Figure 1). Correspondingly, the type of parameters measured reflect the choice of assay. Unfortunately, comparison between the results of different protocols

Correspondence concerning this article should be addressed to P. A. DiMilla, who is currently at the Department of Chemistry, Harvard University, Cambridge, MA 02138.

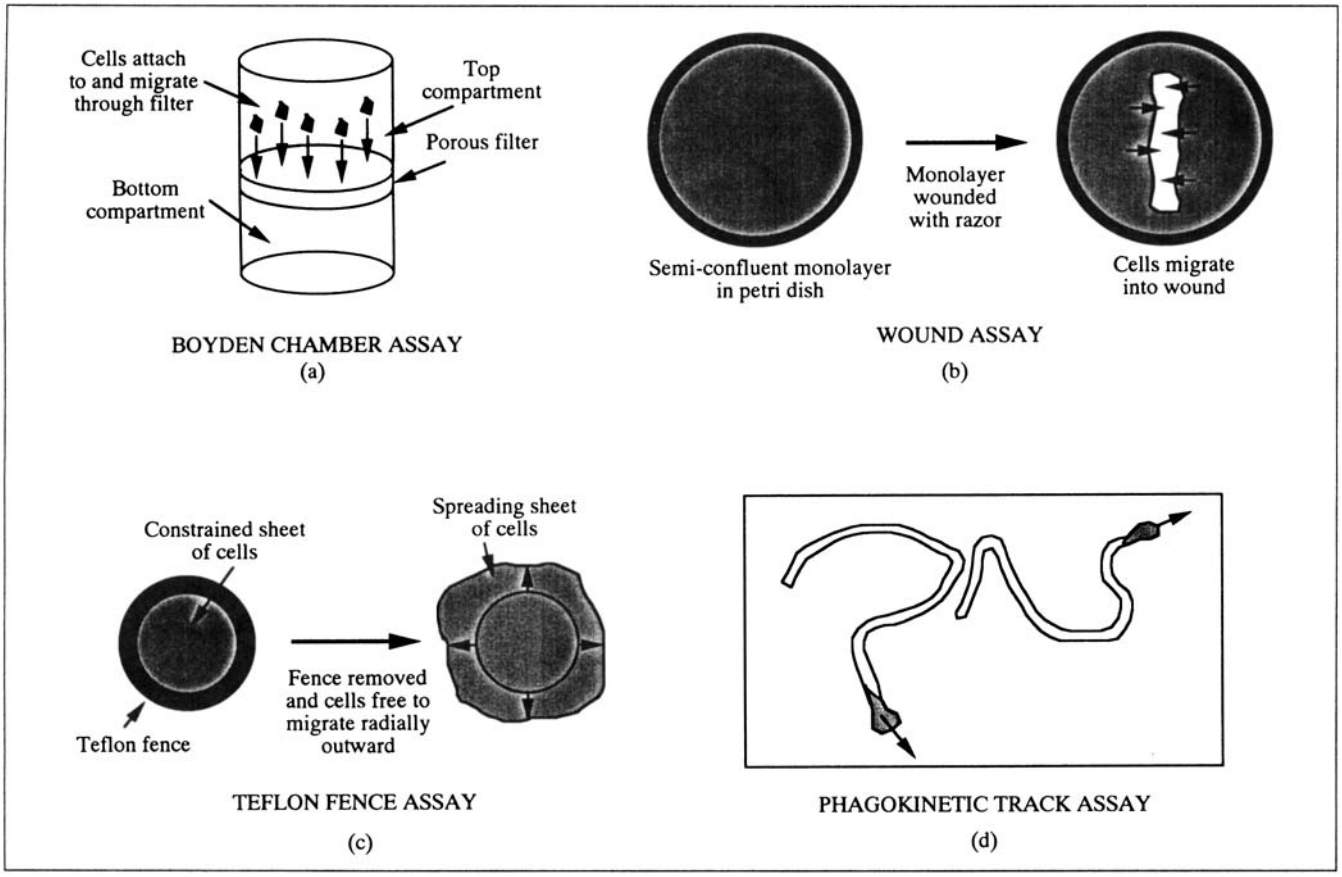

Figure 1. Assays used to measure cell migration.

(a) In the Boyden chamber assay (Boyden, 1962), the number of cells per unit area that reach the bottom of a porous filter is measured; (b) in a wound assay, confluent or semi-confluent cells are wounded and the extent of migration monitored as the number of cells migrating into the wounded area (Sato et al., 1991) or the distance migrated by cells at the leading front into the wound (Majack and Clowes, 1984); (c) in the teflon fence assay, a constrained sheet of cells is freed and the distance migrated by cells at the edge of the expanding sheet measured (Pratt et al., 1984); (d) in the phagokinetic track assay, cells plated on a surface coated with colloidal gold engulf particles as they move, leaving behind particle-free tracks. Migration is measured as the total path distance traveled by each cell after a given time (Lewis and Albrecht-Buehler, 1987) or the average speed, determined by dividing the total distance migrated for each cell by the observation time (Goodman et al., 1989). While techniques a-c examine the motility of a cell population, technique d determines the motility of individual cells.

applied to even the same cell type can be difficult because the empirical parameters typically measured often depend on the physical characteristics of the assay rather than the intrinsic motility of the cells in response to their environment (Lauffenburger, 1983). Further, common assays of cell motility often are inappropriate for providing quantitative measurements of the migration of smooth muscle and other tissue cells, such as fibroblasts and endothelial cells. In isotropic environments these cells behave as persistent random walkers, appearing to move along fairly linear paths over short time intervals but more randomly-oriented paths over longer time intervals (Lackie, 1986), similar to the behavior executed by inert Brownian particles. "Short" and "long" time scales for turning behavior are relative to a persistence time, defined qualitatively as the average time between significant changes in direction of movement. Because typical tissue cells move very slowly, at rates on the order of microns per hour and with persistence times of hours (Gail and Boone, 1970; Dow et al., 1987b; Stokes et al., 1991), measurement of tissue cell movement requires long observation times of many hours to days to distinguish actual translocation from changes in cell morphology, increasing the likelihood that complications from other cellular processes, including proliferation, may affect the measurement.

In recent years the application of time-lapse videomicroscopy to observe the movement of individual cells has received much attention (Dow et al., 1987b). Compared to techniques like the phagokinetic track assay, time-lapse studies are capable of yielding dynamic as opposed to static measurements of cell position and morphology, allowing more information to be obtained in a single experiment (Bodin et al., 1988). In this work we have combined the technique of computer-aided image analysis, which is ideally suited to providing quantitative measurements of cell behavior (Soll et al., 1988), with time-lapse videomicroscopy to determine the trajectories of isolated individual HSMCs on polystyrene petri dishes coated with type IV collagen, fibronectin or laminin. These three molecules are adhesive extracellular matrix (ECM) proteins that form the structural environment these cells experience *in vivo*. Although in the body HSMCs usually form part of a three-dimensional tissue in which cells are in close contact, the isolated cells we have studied here are more amenable to quantitative analysis while two-dimensional surfaces provide a simpler physical environment. [Parkhurst and Saltzman (1992) recently presented a complementary

approach for measuring movement in three-dimensional gels.] By applying a mathematical model describing cell movement as a persistent random walk, we have characterized individual HSMC movement with the two phenomenological parameters cell speed and persistence time. When cell paths are interpreted properly in the context of this model, these quantitative parameters accurately reflect the intrinsic motility of single cells in response to changes in their environment. Further, with unambiguous measurements of these phenomenological parameters we can begin to address questions concerning the relationship between intrinsic cellular properties, extracellular surroundings, and the underlying molecular-level mechanisms responsible for movement (DiMilla et al., 1991b, 1992b).

The main objective of this work is to demonstrate how rigorous quantitative measurements of individual cell speed and persistence time can reveal variations in HSMC movement not apparent based on qualitative observations of the motility of these sluggish tissue cells. To accomplish this goal we have implemented a semi-automated tracking protocol with our image analysis system to identify the paths traveled by isolated HSMCs. Slow-moving tissue cells change shape drastically during movement and require tracking over periods of up to days. Our system, combined with a computer-controlled microscope stage, makes it possible to track a larger number of cells more frequently and over a longer period of observation than in previous studies, allowing sound statistical comparisons to be made. Positive identification of the fraction of motile cells on different substrates complements measurements of speed and persistence time for motile cells. Probabilistic analysis of distributions of persistence time provides data that support the underlying stochastic model for individual cell motility. Our results demonstrate that measurement of means and distributions of phenomenological parameters reflecting the intrinsic motility of individual cells is a valuable technique for examining the effects of surface composition on tissue cell movement *in vitro*.

Materials and Methods

Cell culture

HSMCs, isolated from aortic segments obtained from renal transplant donors, were provided by Dr. Elliot Levine (Wistar Institute, Philadelphia, PA) and cultured as previously described (Tan et al., 1991). Briefly, cells were grown in complete medium composed of medium 199 (Gibco Laboratories, Grand Island, NY) supplemented with 2-mM glutamine and 10% heat-inactivated fetal bovine serum (Gibco) in gelatin-coated tissue-culture flasks and passaged every 6–10 days. Cultures were incubated at 37°C in a humidified CO_2 atmosphere and fed every three to four days with fresh complete medium. Confluent cells exhibited a hill-and-valley appearance characteristic of cultured vascular smooth muscle cells. Cells for migration assays were used between cumulative population doublings of 14.9 and 17.7.

Cells were subcultured by aspirating depleted medium, washing with 0.25% of trypsin/versine (Gibco), and incubating with fresh tryspin/versine at 37°C until cells detached. A fourfold excess of 0.2 wt. % soybean trypsin inhibitor (Worthington Biochemical Corp., Freehold, NJ) in serum-free MCDB-104 medium (Gibco formula #82-5006EA), supplemented with 10-μg/mL gentamicin antibiotic (Sigma Chemical, St. Louis, MO), was added and the resulting suspension of cells spun in a refrigerated centrifuge at 1,500 rpm for 10 minutes. Aggregates of cells were dispersed by pipetting with fresh MCDB-104 medium repeatedly to form a suspension of single cells. Cell concentration was determined electronically with a Model ZM Coulter counter (Coulter Electronics, Inc., Hialeah, FL).

Preparation of cell migration assay

Sterile 35-mm-dia. nontissue culture petri dishes (Falcon #1008, Becton Dickinson Labware, Lincoln Park, NJ) coated with adhesive ECM protein (type IV collagen, fibronectin or laminin) were prepared to observe the motility of isolated individual HSMCs. 1-mg/mL type IV collagen in 1-mM acetic acid (a gift of Dr. Stuart Williams, Thomas Jefferson University, Philadelphia, PA) was diluted into PBS (0.01-M phosphate buffer, pH 7.2, 0.15-M NaCl), while laminin, provided by Dr. Hynda Kleinman (NIH, Bethesda, MD), was dissolved initially in sterile water. Sterile stock solutions of human plasma fibronectin (Boehringer Mannheim, Indianapolis, IN) were prepared by thawing lyophilized 100-μg aliquots in sterile PBS. All proteins solutions were stored at 4°C before diluting in PBS to a final concentration of 10 μg/mL for use.

Petri dishes were incubated with 1.5 mL of ECM protein solution at 10 μg/mL for 24 hours at 4°C. After aspirating the ECM protein solution, 1.5 mL of a sterile 1 wt. % solution of heat-denatured bovine serum albumin (BSA, Fraction V, 96–99% albumin, Sigma), prepared as described by DiMilla et al. (1992a), was added to each dish for 45 minutes at room temperature to block nonspecific adhesion between cells and underlying plastic. The BSA solution then was aspirated and the dish washed successively three times with sterile PBS at room temperature to remove unadsorbed protein before cells were added.

Cells were added at $1\text{–}2 \times 10^3$ cells/cm^2 in 2 mL of serum-free MCDB-104 medium. These sparse densities maximized the number of cells in a given microscopic field of observation while minimizing the probability of cell-cell encounter. Observing the cells in serum-free medium prevented the adsorption of additional attachment factors present in serum onto the underlying substrate, allowing observation in a better-defined chemical environment. We maintained pH in the physiological range of the microscope stage in the absence of a humidified 5% CO_2-atmosphere enclosure by adding 25-mM HEPES (N-2-hydroxyethylpiperazine-N′-2-ethanesulfonic acid, sodium salt, Sigma Chemical) to the bicarbonate-free medium. Each dish then was sealed with two strips of Parafilm to minimize evaporation of medium. The dishes were placed in an incubator at 37°C overnight to allow the cells to settle to the bottom of the dish, stably attach, and spread.

Time-lapse videomicroscopy and image analysis

For each experiment a prepared petri dish with adherent cells was placed on the stage of a Zeiss Axiovert 10 inverted microscope equipped with a Phase 1 Achrostigmat 10×/0.25 NA objective and LD 0.3 NA long-working distance condenser (Carl Zeiss, Inc., Thornwood, NY). Cell movement was observed under phase-contrast optics using a green neutral-contrast filter and a Hamamatsu C2400 videocamera (Photonic Microscopy, Inc., Oak Brook, IL). At a total magnification at the videocamera face plate of 100×, each field of view contained 8–10 cells on average. To observe appreciable cell

movement during the course of each experiment, we recorded video images continuously for two to three days at 1/120th of real time using a JVC Model BR-9000U time-lapse VCR (JVC Company of America, Elmwood Park, NJ). During each experiment the current date and time were recorded continuously on the lower half of the screen by the digital date-time generator of the BR-9000U. Temperature on the microscope stage was maintained at 37°C using an ASI 400 Air Stream Incubator (Nicholson Precision Instruments, Inc., Gaithersburg, MD) and varied less than two degrees over the petri dish surface during the course of an experiment. Cell movement was recorded only after the petri dish had been on the stage at least one-half hour.

To enhance our ability to gather data during a single experiment, we used a Mertzhauser IM-EK32 motorized microscope stage (Opto-Systems, Inc., Newtown, PA), controlled by a MAC 1000 controller (Ludl Electronic Products, Hawthorne, NY), to sample multiple target positions sequentially on a petri dish during a single experiment. Between 15 and 60 target fields were selected manually with a joystick by serpentinely scanning the petri dish (to avoid choosing the same cell or field multiple times). Care was taken to avoid field selection based on cell morphology, such as size or shape. During an experiment each target field was videotaped sequentially for at least 15 seconds once every 15 minutes. Accuracy in stage resolution and timing has been validated previously (DiMilla, 1991).

Movement of HSMCs in each target field was followed by playback of videotapes through an image processing system consisting of a FA-400 digital time-base corrector (FOR-A Corporation of America, Boston, MA), a Series 151 real-time image processor (Imaging Technology, Inc., Woburn, MA), and a PC-AT 286 microcomputer (AST Research, Inc., Irvine, CA). Basic image processing operations were implemented using library functions in the TIPS-151 package (Mnemonics, Inc., Mt. Laurel, NJ) especially designed for the Series 151 processor. We applied this system to track the position of cell centroids at intervals of $\Delta t = 15$ min using a semi-automated algorithm in which a single field was analyzed at a time. This algorithm combined the speed of a box-search algorithm (Dow et al., 1987b) with the flexibility of manual tracking. Only isolated and spread cells that were not in contact with other cells and were fully contained within the field of view were tracked at each interval. Centroids for many cells could be identified based on the white centroids of rectangles enclosing images of each cell after image binarization, limiting user involvement to simply advancing the videotape manually and ascertaining whether each cell was spread, isolated, and fully on-screen. However, even cells that possessed highly nonuniform phase halos could be followed manually by placing a keyboard-controlled cursor. This latter feature proved useful especially for tracking cells in fields that were poorly focused or unevenly lit. The pixel coordinates of each cell centroid $\{x(n\Delta t), y(n\Delta t)\}$ were recorded at each elapsed tracking interval $n\Delta t$ for further analysis. Each field was analyzed for up to 48 hours. Further details of this tracking procedure have been discussed elsewhere (DiMilla, 1991).

Analysis of experimental cell paths with persistent random walk model

Qualitative differences in individual cell paths were interpreted quantitatively by describing the movement of isolated cells as a correlated or persistent random walk. Based on independent theoretical treatments, Dunn (1983), Othmer et al. (1988), and Alt (1990) have proposed that the average squared displacement $<\boldsymbol{d}\cdot\boldsymbol{d}>$ over time t of a cell moving in an isotropic environment depends only on two parameters, cell speed S and persistence time P:

$$<\boldsymbol{d}\cdot\boldsymbol{d}> = 2S^2P[t - P(1 - e^{-t/P})]. \tag{1}$$

Dunn (1983) proposed Eq. 1 by approximating the curvilinear path of a moving cell as a series of discrete segments over a constant time interval τ and defined P as the directional persistence of the cell. In contrast, Othmer et al. (1988) derived Eq. 1 assuming that while cell speed and orientation are regulated by separate underlying mechanisms, changes in cell velocity occur randomly according to a Poisson process with intensity λ. In their formalism, P is actually a persistence in velocity rather than direction alone and a function of both the frequency of velocity changes and choice of movement direction:

$$P = \frac{1}{\lambda(1 - \psi_d)}. \tag{2}$$

where the index of directional persistence ψ_d, representing the mean directional cosine, is a direct measure of a cell's persistence in direction. Recently, Alt (1990) derived Eq. 1 based on velocity autocorrelation functions.

Equation 1 exhibits behavior characteristic of both a wave propagation process with propagation speed S for $t \ll P$ and a diffusive process with diffusivity:

$$\mu = \frac{\overline{S}^2\overline{P}}{n}, \tag{3}$$

where $\overline{S}$ and $\overline{P}$ are mean speed and persistence time, respectively, and n is the dimensionality of the environment for $t \gg P$ (Alt, 1980; Othmer et al., 1988; Rivero et al., 1989). The parameter μ, the random motility coefficient, characterizes the motility of a cell population (Keller and Segel, 1971). Values of μ calculated based on values for the individual cell motility parameters speed and persistence time and Eq. 3 can be compared with measurements determined directly from assays of cell population motility (Lauffenberger, 1983).

We calculated the average-squared displacement as a function of time interval $n\Delta t$ for each cell using the spatial coordinates obtained from image processing. Displacements were converted from pixels to microns with the factor $C = 0.21$ x-pixels/microns, measured using a calibration slide. Because each pixel was 25% longer in the x direction than in the y direction, squared displacements from $\{x(t),\ y(t)\}$ to $\{x(t+i\Delta t),\ y(t+i\Delta t)\}$ were calculated as:

$$\boldsymbol{d}\cdot\boldsymbol{d}_{t-t+i\Delta t} = C^{-2}\left[[x(t+i\Delta t) - x(t)]^2 + \left[\frac{y(t+i\Delta t) - y(t)}{1.25}\right]^2\right]. \tag{4}$$

To take advantage of all positional information available,

overlapping intervals were used. Thus, the mean-squared displacement at a time interval of $t_d = n\Delta t$ for a cell tracked for a total of $t_{max} = N\Delta t$ minutes was:

$$<\boldsymbol{d}\bullet\boldsymbol{d}(t_d = n\Delta t)> = \frac{1}{(N-n+1)}\sum_{i=0}^{N-n}\boldsymbol{d}\bullet\boldsymbol{d}_{i\Delta t\rightarrow(n+i)\Delta t}. \quad (5)$$

Similarly, variances in squared displacement were determined (for $t_d \neq t_{max}$) as:

$$\sigma^2_{d\bullet d}(t_d = n\Delta t) = \frac{1}{N-n}\sum_{i=0}^{N-n}[\boldsymbol{d}\bullet\boldsymbol{d}_{i\Delta t\rightarrow(n+i)\Delta t} - <\boldsymbol{d}\bullet\boldsymbol{d}(t_d)>]^2. \quad (6)$$

For each cell we attempted to fit the experimental data for mean-squared displacement as a function of time to Eq. 1 with cell speed S and persistence time P as adjustable parameters using the Levenberg-Marquardt method for nonlinear least squares fitting (Press et al., 1986). Experimental data for $<\boldsymbol{d}\bullet\boldsymbol{d}>$ for time intervals less than $t_{min} = 4\Delta t = 60$ minutes or greater than $t_d = t_{max}/2$ ($n = N/2$) were not included in the fitting procedure: over very short intervals uncertainties in centroid location obscure actual movement, while over very long intervals insufficient intervals are available for averaging. Paths for cells that were followed less than 6 hours were not analyzed.

No previous model for cell movement provides criteria for distinguishing motile from immotile cells. Intuitively, an immotile cell will exhibit a negligible displacement relative to its characteristic length over long observation times. Further, a persistence in direction will not be observed. To interpret the behavior of our real tissue cells, as a threshold we set a $P_{min} = 30$ min as a realistic minimum persistence time for two reasons: first, at a magnification of $C = 21$ x-pixels/100 micron and typical tissue cell speeds on the order of fractions of micron/min, uncertainties in locating cell centroids would obscure movement at shorter persistence times using a sampling time of $\Delta t = 15$ min; secondly, persistence phenomena in large tissue cells, such as HSMCs, arise from rearrangements in internal cellular structures with kinetics on the order of tens of minutes (Singer and Kupfer, 1986). If Eq. 1 were valid for a cell moving with $P = P_{min}$, then for $t_{min} < t < t_{max}/2$

$$D^2_{max}(t) \equiv \frac{t - P_{min}(1 - e^{-t/P_{min}})}{\frac{t_{max}}{2} - P_{min}(1 - e^{-t_{max}/2P_{min}})}. \quad (7)$$

Values of $<\boldsymbol{d}\bullet\boldsymbol{d}(t)>$ greater than $D^2_{max}(t)\bullet<\boldsymbol{d}\bullet\boldsymbol{d}(t_{max}/2)>$ can occur only for $P < P_{min}$ (DiMilla, 1991). Thus, as an operational criterion we defined an immotile cell as a cell in which more than 35% of the time intervals for $t_{min} \leq t_d \leq t_{max}/2$ have mean-squared displacements greater than the corresponding value of $D^2_{max}(t_d)\bullet<\boldsymbol{d}\bullet\boldsymbol{d}(t_{max}/2)>$ for that time interval. Although the choice of a 35% cutoff is arbitrary, the application of this criterion to distinguish immotile from motile cells was not sensitive to the exact cutoff value. Cells which passed this criterion with fitted persistence times less than P_{min}, along with those cells with $P > t_{max}/3$, were excluded from further analysis.

For each substrate means and standard errors in the mean for cell speed were calculated based on best-fit values for all cells (motile and immotile) observed on that substrate, while the corresponding statistics for persistence time were calculated using values only from motile cells. Using Eq. 3 statistics for the random motility coefficient μ were calculated based on means and standard deviations for speed and persistence time averaged over motile cells only and with dimensionality $n = 2$. Finally, we determined the population parameter % motile cells as the percentage of the total number of cells observed on a substrate that were motile. Standard deviations for this parameter were estimated by assuming a binomial distribution described the observation of motile cells. Parameter values among different ECM substrates were compared using the unequal variance Student's t-test (Devore, 1991).

Statistical analysis of distributions of individual cell parameters

Experimental number distributions of cell speed were determined by counting the number of cells with best-fit values for speed falling within 7.5 micron/h-wide bins for each ECM substrate type and plotted vs. the intermediate value for speed for each bin. Immotile cells were excluded from this analysis. For comparison normal probability distributions were calculated with the mean $\bar{S}$ and standard deviation σ_S in speed for motile cells as:

$$f(S) = \frac{1}{\sqrt{2\pi}\sigma_S}e^{-(S-\bar{S})^2/2\sigma_S^2} \quad (8)$$

and plotted with experimental number distributions by multiplying by the total number of motile cells observed and bin size.

Experimental number distributions of persistence times were determined similarly by pooling experimental measurements of persistence time into 1 h-wide bins and plotted at the intermediate value of persistence time for each bin. These experimental number distributions were compared to the exponential interarrival-time probability distribution (Devore, 1991):

$$f(P,\lambda) = \lambda e^{-\lambda P}, \quad (9)$$

where the parameter $\lambda > 0$ is the intensity of an underlying stationary Poisson process. We estimated a value for λ for each ECM substrate by a linear least-squares fit of the natural logarithm of the complement of the cumulative exponential probability distribution F_c:

$$\ln[F_c(P,\lambda)] = -\lambda P, \quad (10)$$

to the logarithm of the complement of the cumulative experimental number distribution, calculated by summing the number of cells with persistence times greater than or equal to the minimum persistence time for each bin and dividing by the total number of motile cells observed. Nonzero values for the fitted y-intercept were observed because bins of finite size were used, very short persistence times were not measurable, and limited numbers of motile cells were sampled. Outlier points, which resulted from the measurement of a very small number of long persistence times, were excluded from the least-squares analysis.

Results

Qualitative observations of individual HSMC motility

With our time-lapse videomicroscopy system we observed spread vascular HSMCs that usually were bipolar and elongated by 18 hours after plating, with lengths of approximately 50-100 micron. Cells did not behave as hard elastic particles upon collision but rather adhered to each other. Groups of cells in contact did not translocate significantly but frequently separated after contact, often persisting in their previous direction of movement. Some cells also rounded up during the course of an experiment but were otherwise indistinguishable from spread cells. Loss of directional polarity accompanied rounding up.

Both obviously motile and apparently immotile cells changed morphology dramatically over a period of hours and thus could not be distinguished based solely on cell size or shape. On a time scale of minutes cell movement appeared as a saltatory cycle of lamellipod extension at the leading edge followed by retraction of the cell's tail. During lamellipodal extension, the body of the cell remained relatively stationary. Tail retraction was more abrupt and less smooth than lamellipodal progression and, especially for rapidly moving cells, sometimes resulted in the deposition of fragments on the substratum where the uropod had been previously. Although most cells turned smoothly through lamellipodal extensions at the front with little accompanying activity at the rear, some cells were observed to change direction abruptly, appearing to be unpolarized during this process. In contrast, apparently immotile cells often extended blebs (pseudopods) around their periphery without establishing a preferred direction for movement.

Quantitative description of individual HSMC motility

To obtain quantitative measures of intrinsic single HSMC motility from our time-lapse recordings, we followed the movement of isolated cells with our computer-controlled image analysis system and semi-automated tracking program. Given centroid position as a function of time, we could reproduce the paths traveled by isolated single cells in a field over the course of an experiment by linking the discrete position of the centroid at intervals of $\Delta t = 15$ min. In contrast to the observations of Dow et al. (1987b), we did not notice systematic differences in the smoothness of the cell paths for cells tracked with either the fully-automated or manual features of our protocol. In Figure 2 we show cell paths for three typical cells tracked over 48 hours. From these paths it is obvious that cell 3 did not translocate compared to cells 1 and 2 and that cell 2 moved further than cell 1 over the two-day period. The movement of cells 1 and 2 also is qualitatively consistent with the behavior expected for a persistent random walker: over a time scale of a few hours each cell tended to persist in its direction of movement, while over longer times the direction of movement was more random. In contrast, cell 3 showed no persistence in movement in any direction.

Qualitative differences in migration between cells could be compared quantitatively by analyzing their movement in the context of the persistent random walk model. Applying Eqs. 5 and 6 we calculated both the mean and standard deviation in squared displacement, $<d \cdot d>$ and $\sigma_{d \cdot d}$, respectively, as a function of time interval from the cell paths for cells 1, 2, and 3 (Figure 3). As expected, cell 2 had larger values of $<d \cdot d>$ over time compared to cell 1. In contrast, cell 3 exhibited mean-squared displacements more than one and two orders of magnitude smaller than cells 1 and 2, respectively. Also, the standard deviations in squared displacement for cells 1 and 2 increased over time for intervals less than approximately 25 hours, while values for $\sigma_{d \cdot d}$ remained relatively constant but noisy for cell 3: the correlation between displacements faded over longer time intervals for cells 1 and 2 than for cell 3. For all three cells these standard deviations decreased toward zero for long interval times because fewer intervals were available for analysis and these overlapping intervals were less statistically independent.

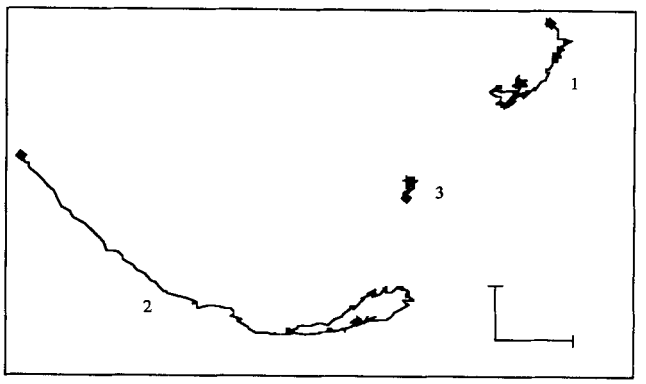

Figure 2. Cell paths for three typical isolated HSMCs over 48 hours.

Motile behavior of isolated individual cells was recorded using time-lapse videomicroscopy and cell centroid position tracked using an image processor and a semi-automated tracking algorithm. Continuous paths were formed by linking centroid coordinates at 30-min intervals; ♦ = starting position for each cell, — = 100 micron.

For cells 2 and 3 we fit Eq. 1, describing the nonlinear relationship between $<d \cdot d>$ and observation time t for a persistent random walker, to our experimental data with the intrinsic single-cell motility parameters speed S and persistence time P. Values for S and P, fit by least-squares analysis using only data for time intervals between 60 min and 1,440 min (1 day) inclusive, were 8.4 micron/h and 3.5 hours for cell 1 and 27.3 micron/h and 2.2 hours for cell 2, respectively. In Figure 3 we compare the behavior of Eq. 1 using these best-fit estimates of S and P with the experimental data. There was excellent agreement between experimental and theoretical curves over a large range of times, from $t < P$ to $t \gg P$ (given values of P on the order of a few hours). In particular, the experimental data for 1 h $< t <$ 30 h is consistent with the linear moderately-large time expression for $t \gg P$ derived by Gail and Boone (1970):

$$<d \cdot d> = 4\mu[t - P]. \tag{11}$$

Disagreement at longer times arose because not enough intervals were averaged to yield reliable means in squared displacement. Fits were more sensitive to perturbations in speed than persistence time. Note that although cell 2 moved more than three times as fast as cell 1, as would be predicted intuitively from the corresponding cell paths, the former cell had a shorter persistence time compared to the latter. This difference in turning behavior is not obvious from examination of the cell paths.

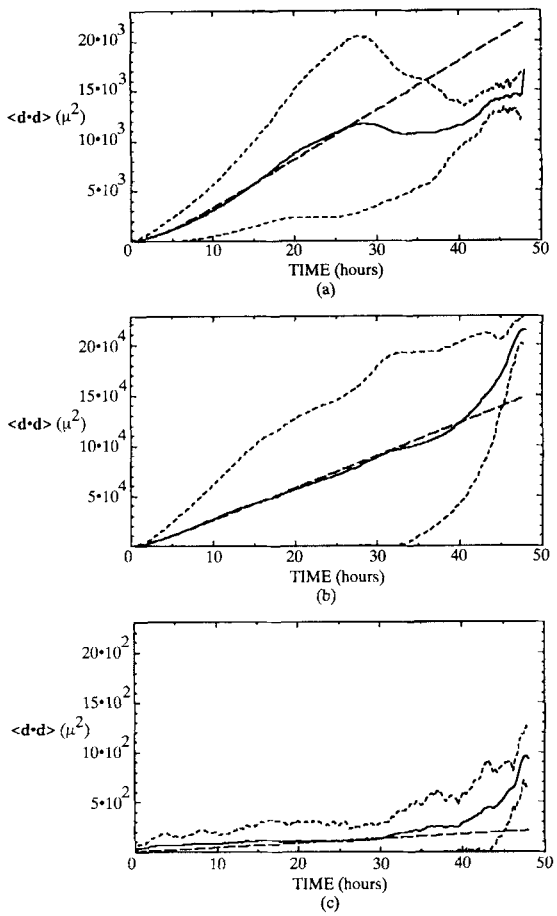

Figure 3. Mean-squared displacement vs. time for three isolated HSMCs whose cell paths over 48 hours are in Figure 2: (a) cell 1; (b) cell 2; (c) cell 3.

Average-squared displacements $<d \cdot d>$ and standard deviations $\sigma_{d \cdot d}$ as a function of interval time were calculated from cell paths using overlapping intervals and Eq. 5. A nonlinear theoretical model for a persistent random walk (Eq. 1) was fit to the experimental data with the adjustable parameters root-mean-squared speed S and persistence time P for cells 1 and 2. Solid curves and curves with shorter dashes depict experimental mean-squared displacements and means ± one standard deviation in squared displacement, respectively. Equation 1 with best-fit values for S and P (8.4 micron/h and 3.5 h for cell 1 and 27.3 micron/h and 2.2 h for cell 2, respectively) are represented by curves with longer dashes in a and b, while Eq. 7 scaled by $<d \cdot d(t = 24 \text{ h})> = 106$ micron^2 is plotted with the longer dashes in c. Cell 3 was classified as immotile and assigned a speed of 0 micron/h and persistence time undefined.

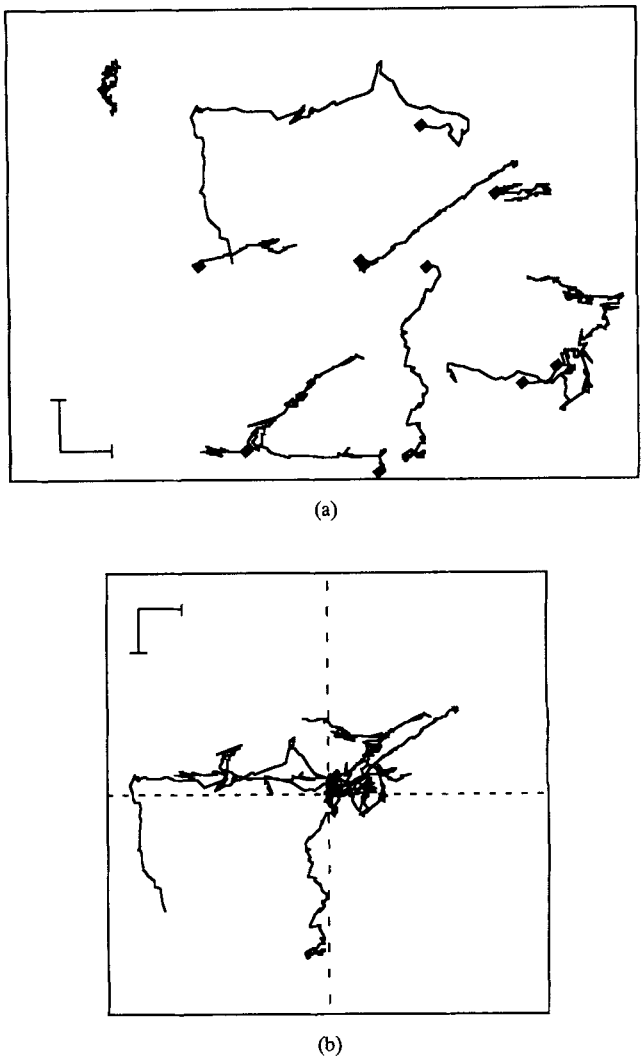

Figure 4. Typical cell paths for HSMCs on 10-μg/mL type IV collagen: (a) paths of cells tracked in a single field; (b) paths superimposed to a common starting point in a "wind-rose" display.

Individual cell motile behavior was recorded using time-lapse videomicroscopy for cells on nontissue culture petri dishes coated with type IV collagen. Continuous paths of centroid position every 30 min were traced for ten isolated cells tracked using an image processor and a semi-automated tracking algorithm; ♦ = starting point for each cell; — = 100 micron.

In contrast, for cell 3 there was poor correspondence between experimental values for $<d \cdot d(t)>$ and the theoretical model for individual cell movement. In Figure 3c we plot Eq. 7 scaled by $<d \cdot d(t_{max}/2 = 24 \text{ h})> = 106$ micron^2. This curve lies almost entirely below the experimental data, so that based on our criteria for quantitatively distinguishing motile from immotile cells, cell 3 did not actually exhibit true translocation.

The vast majority of cells we examined could be characterized as either motile (assigned positive speeds and finite persistence times) or immotile (assigned speeds of zero and persistence times undefined) based on analysis of their mean-squared displacements over time. Since we have measured speeds for HSMCs as low as 1 micron/h with our analysis (data not shown), the possibility that "immotile" cells actually moved at a speed below some measurable threshold is unlikely. In general, the results of our quantitative criteria for identifying immotile cells agreed with perceptions of cell movement based on examining cell paths qualitatively. However, a few cells appeared to stop and "rest" during the course of an experiment. Because the persistent random walk model assumes that cell speed is constant and not a function of observation time, movement of these cells could not be interpreted with this model. Also, data for cells with fitted values of $P > t_{max}/3$ was unreliable because these cells were tracked for an insufficient length of time to obtain accurate estimates of directional persistence (Stokes et al., 1991). There was no systematic variation in the number of resting cells or cells with extremely large

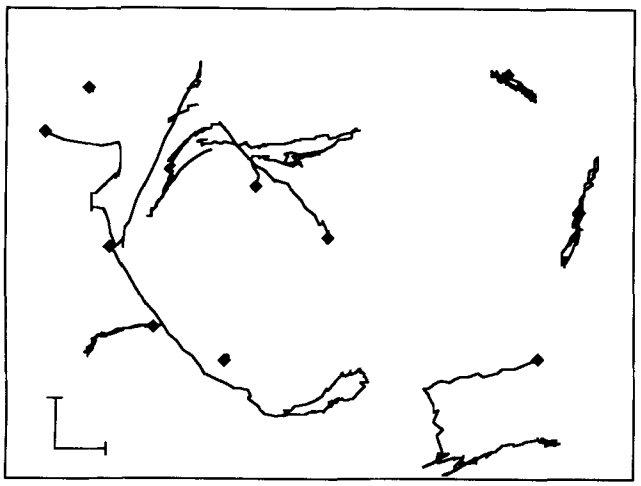

(a)

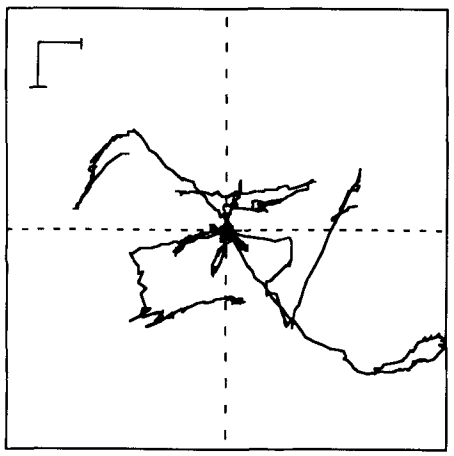

(b)

Figure 5. Typical cell paths for HSMCs on 10-μg/mL fibronectin.

Description is the same as Figure 4 except that fibronectin was used instead of type IV collagen; — = 100 micron.

(a)

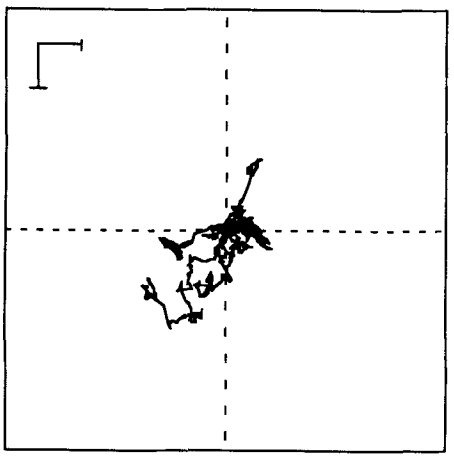

(b)

Figure 6. Typical cell paths for HSMCs on 10-μg/mL laminin.

Description is the same as Figure 4 except that laminin was used instead of type IV collagen; — = 100 micron.

values of fitted P with experimental conditions, justifying the exclusion of these cells from subsequent statistical analysis.

Individual HSMC motility parameters on different ECM-coated surfaces

We applied our approach for measuring individual cell motility to examine the possible effect of substratum composition on HSMC migration. Although previous studies have indicated that the concentration of ECM proteins adsorbed to a surface can influence the locomotion of skeletal muscle myoblasts (Goodman et al., 1989) and fibroblasts (Straus et al., 1989), these studies were not based on rigorous measurement of parameters describing intrinsic cell movement rate or turning behavior. Using our time-lapse videomicroscopy system we recorded the behavior of HSMCs on nontissue-culture petri dishes which had been coated with 10 μg/mL type IV collagen, fibronectin or laminim. Albelda et al. (1989) showed that the initial adhesion of cultured human endothelial cells reached a maximum at these concentrations. We tracked between six and nine fields from duplicate experiments for each substrate type. Cell paths over a 48-hour period for sample fields on each of these substrates are depicted in Figures 4a, 5a and 6a, respectively. Each field contains ten cells that remained isolated and spread within the field during the experiment. While in each field some cells moved as persistent random walkers, other cells in the same fields did not appear to translocate at all. Although some cells crossed the paths of other cells, we did not observe preferential tracking of one cell along the path taken by another in any field examined.

To compare cell paths between these three substrates more easily, we superimposed the starting position of each cell in the sample fields to a common origin (Figures 4b, 5b and 6b). These "wind-rose" displays (Goodman et al., 1989) demonstrate that the cells did not all move preferentially in one direction, a phenomenon that would be expected for directed cell movement by chemotaxis or haptotaxis but not for random motility in a macroscopically isotropic environment. Means and standard errors in the mean for cell speed and persistence time and means and standard deviations for the fraction of motile cells on each substrate for six to nine fields

Table 1. Motility of HSMCs on ECM-Coated Surfaces

Substrate Type	Cells Analyzed	Individual Cell Parameters*		Cell Population Parameters*	
		Cell Speed (micron/h)	Persistence Time (h)	% Motile Cells	Random Motility Coefficient (cm^2/s)
Type IV Collagen	77 ($n=8$)	11.9 ± 1.0	2.9 ± 0.3	77.9 ± 4.7	$9.5\times10^{-10} \pm 1.6\times10^{-10}$
Fibronectin	62 ($n=9$)	12.5 ± 1.5	3.5 ± 0.6	66.1 ± 6.0	$1.8\times10^{-9} \pm 4.0\times10^{-10}$
Laminin	34 ($n=6$)	13.4 ± 2.7	2.2 ± 0.4	64.7 ± 7.0	$1.3\times10^{-9} \pm 4.9\times10^{-10}$

* Determined for HSMCs migrating on nontissue-culture petri dishes coated with 10 μg/mL ECM protein for 24 hours at 4°C. Root-mean-squared cell speed S and persistence time P were fit to experimental data by applying a persistent random walk model for cell movement, while the fractions of motile cells % motile cells were determined as in the text. Mean speed for all cells observed (assigning each immotile cell a speed of 0 micron/h) and mean persistence for motile cells are reported. Random motility coefficients μ were calculated from mean individual cell motility parameters for motile cells using Eq. 3. Parameter values are presented as mean and standard errors in the mean (standard deviations for % motile cells) based on individual cell data from n fields in duplicate experiments.

from duplicate experiments are summarized in Table 1. Cells speeds averaged over both motile and immotile cells on the three substrates were not statistically different based on a Students' t-test. Although the fields presented in Figures 4-6 suggest that cells on laminin migrated less than those on collagen or fibronectin, many cells on laminin were tracked for less than 48 hours and moved at rates comparable to those on the other two substrates. In contrast, persistence times on fibronectin were more than 60% longer than those on laminin and 20% longer than those on collagen; the greater persistence times on fibronectin were statistically significant compared to persistence time on laminin but not persistence time on type IV collagen (based on 95% confidence level from Student's t-test). Further, a statistically-significant greater fraction of cells moved on collagen compared to the other two substrates (>95% confidence level from Student's t-test). From the individual motile cell means for speed and persistence time, random motility coefficients on the order of 10^{-9} cm^2/s were calculated for each substrate. Variations in random motility coefficient among the substrates reflect a combination of the trends exhibited by cell speed and persistence time. We note that further interpretation of differences in motility parameters is unwarranted because even though each surface was coated with the same soluble concentration of ECM protein, the actual absorbed surface density can depend on the particular protein studied (DiMilla et al., 1992a).

Distribution of individual HSMC motility parameters

We also were interested in how distributions of the individual cell parameters speed and persistence time might vary among substrate types. Number distributions of cell speed for motile cells on type IV collagen, fibronectin and laminin using 7.5 micron/h wide bins are shown in Figure 7. The distributions for collagen- and fibronectin-coated surfaces were consistent with a normal distribution (Eq. 8). In constrast, the speed distribution on laminin demonstrated poorer agreement with the theoretical distribution. This discrepancy, however, resulted at least partially from the smaller number of motile cells tracked on the latter substrate.

Analysis of persistence time distributions provided a valuable tool for characterizing the turning behavior of motile cells. Number distributions of persistence times for HSMCs on each substrate, determined using 1-h-wide bins, were comparable to exponential probability distributions (Eq. 9 and Figure 8). Observation of additional motile cells, especially on fibronectin and laminin, probably would have removed the few outlier

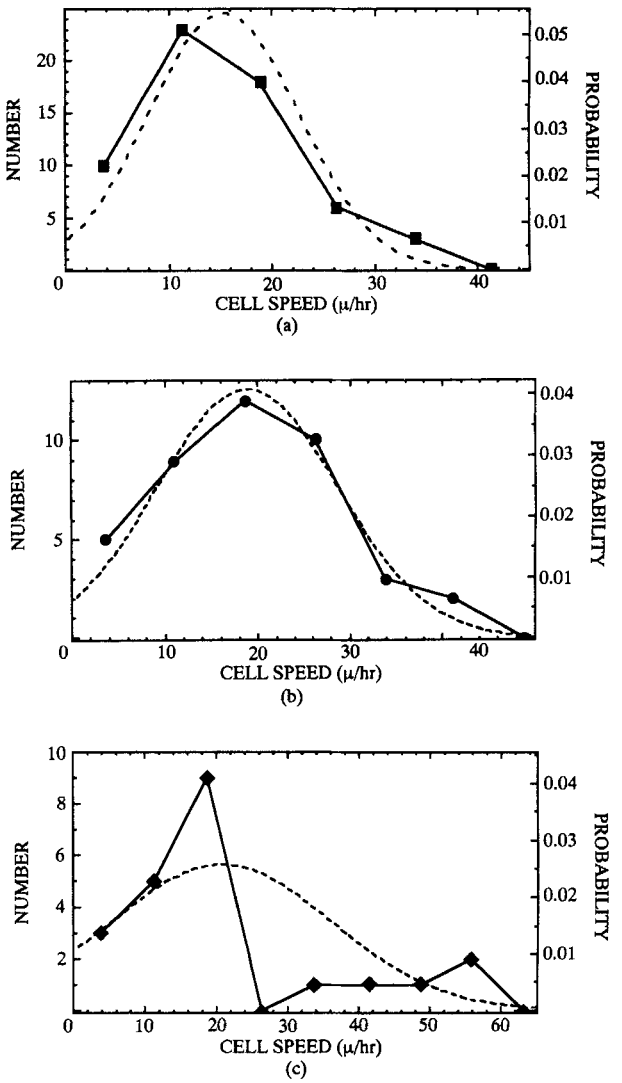

Figure 7. Distributions of cell speed for HSMCs on nontissue culture petri dishes coated with 10-μg/mL ECM protein: (a) type IV collagen; (b) fibronectin; (c) laminin.

The number of motile cells with speeds within 7.5 micron/h-wide bins from 6 to 9 fields in duplicate experiments were counted. Numbers for each bin are plotted at the intermediate speed for the bin as filled symbols connected with solid lines. Normal probability distributions (Eq. 8) based on the mean and standard deviation in speed for motile cells were normalized for the number of cells observed and bin size and are plotted as dashed lines.

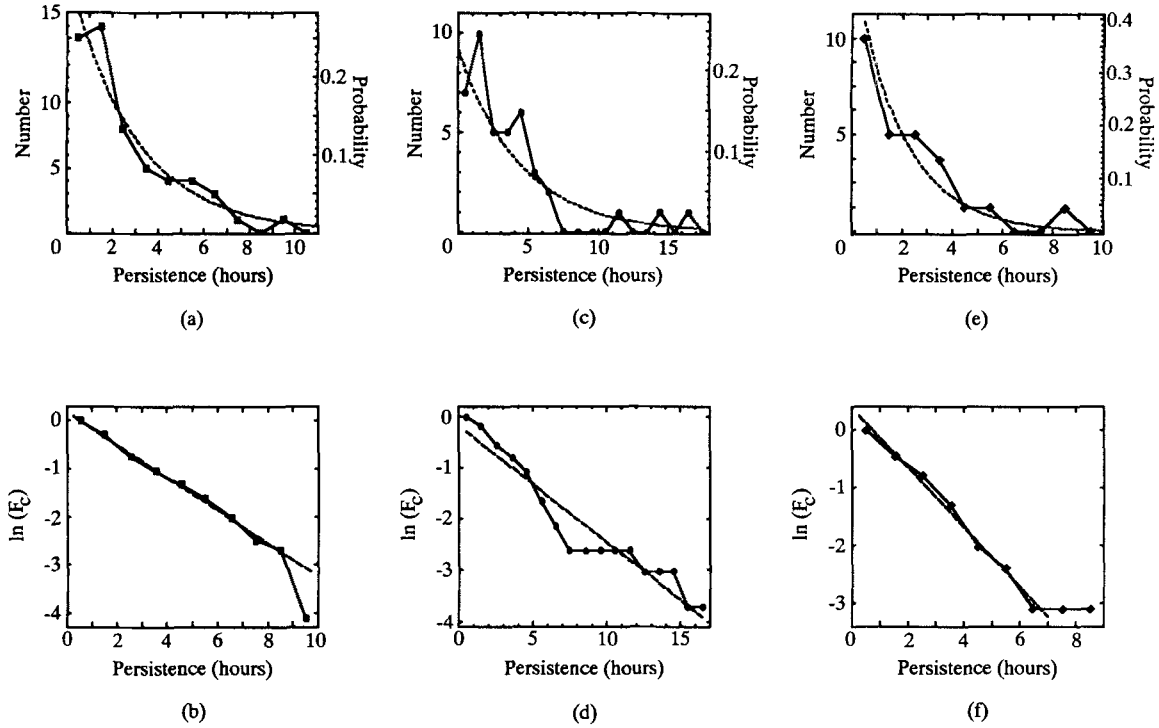

Figure 8. Distributions of persistence times for HSMCs on nontissue culture petri dishes coated with 10-μg/mL ECM protein.

The number of motile cells with persistence times within 1-h-wide bins from 6 to 9 fields in duplicate experiments were counted. Experimental number distributions for persistence time on type IV collagen (■), fibronectin (●) and laminin (◆) are plotted at the intermediate persistence time for each bin, connected with solid lines, in a, c, and e, respectively. Exponential probability distributions for motile cells (Eq. 9) based on the parameter $\lambda = 0.344\ h^{-1}$ for type IV collagen, $0.226\ h^{-1}$ for fibronectin, and $0.513\ h^{-1}$ for laminin were normalized for the number of cells observed and bin size, and are plotted as dashed lines in these same figures. Complement cumulative experimental number distributions were calculated as the fraction of cells with persistence times ≥ minimum persistence time for each 1-h bin. These distributions are plotted on a logarithmic scale vs. the intermediate persistence time for each bin as squares for type IV collagen (b), circles for fibronectin (d), and diamonds for laminin (f), connected by solid lines. Linear least-squares fits of the experimental data (with the exclusion of the outlier points for $P_{min} = 9$–10 h for type IV collagen and $P_{bin} = 7$–8 and 8–9 h for laminin), representing Eq. 11, are depicted by dashed lines with slope $-0.344\ h^{-1}$ and y-intercept 0.184 for type IV collagen, slope $-0.226\ h^{-1}$ and y-intercept 0.187 for fibronectin, and slope $-0.513\ h^{-1}$ and y-intercept 0.364 for laminin.

points in Figures 8b and 8f. Each number distribution could be described by a single parameter λ, whose reciprocal was by definition both the mean and standard deviation in persistence time. We determined values of λ for each substrate by fitting the logarithm of a complement cumulative exponential distribution (Eq. 10) to the logarithm of its corresponding experimental distribution found by calculating the fraction of cells with persistence times ≥ minimum persistence time for each 1-h bin. Given the fitted values for λ there was excellent agreement between exponential and experimental number distributions for persistence times on collagen and laminin, while distributions on fibronectin were less comparable yet not inconsistent.

In Table 2 we compare our estimates for mean and standard deviations in persistence time calculated using standard definitions of these two statistics with estimates from the exponential distribution analysis. Even with the limited numbers of motile cells (only 22 motile cells were observed on laminin), for cells migrating over collagen- and laminin-coated substrata there was excellent agreement between means and deviations measured directly and those measured based on an underlying exponential distribution. Although there was poorer agreement for the two sets of statistics for cells on fibronectin, this discrepancy was expected since the match between theoretical and experimental number distributions was poorer on this substrate. However, standard deviations in persistence time were within 80% of the corresponding mean on all three substrates, with even better agreement for cells on fibronectin-coated surfaces.

Discussion

We have presented an experimental approach for characterizing the intrinsic random motility of slow-moving individual tissue cells, such as the HSMCs examined here, in isotropic two-dimensional environments. Using time-lapse videomicroscopy and semi-automated image analysis, we tracked the paths traveled by isolated single HSMCs over a period of up to two days. By applying a mathematical model describing individual cells as persistent random walkers (Eq. 1), we determined both means and distributions for the two phenomenological parameters cell speed and persistence time for HSMCs on surfaces coated with type IV collagen, fibronectin or laminin, a series of adhesive ECM proteins that these cells encounter in the human body. We emphasize that quantitative measurements of tissue cell migration provided by our ap-

Table 2. Comparison between Normal Statistical and Exponential Distribution Analyses for Persistence Time*

Substrate Type	Cells Analyzed	Standard Statistics for Persistence Time (h)	Distribution Analysis Statistics for Persistence Time (h)
Type IV Collagen	60 ($n=8$)	2.9±2.4	2.9±2.9
Fibronectin	41 ($n=9$)	3.5±3.6	4.4±4.4
Laminin	22 ($n=6$)	2.2±2.0	2.0±2.0

* Persistence times for motile isolated cells on nontissue culture petri dishes coated with 10-μg/mL type IV collagen, fibronectin or laminin for 24 h at 4°C were determined as best-fit values between a persistent random walk model and experimental data for mean-squared displacement as a function of time. Results are reported as means ± standard deviations of cells in n fields in duplicate experiments. Standard statistics were calculated based on the definitions of the mean and standard deviation of individual cell values. Distribution analysis statistics determined by assuming an exponential distribution describes experimental number distributions of persistence times and calculating the exponential probability distribution parameter λ from linear least-squares fits of a complement cumulative exponential distribution to experimental complement cumulative number distributions (see Figure 8). Given an underlying exponential distribution, the reciprocal of λ equals both the mean and standard deviation in persistence time.

proach, based on observation of large numbers of individual cells, are more rigorous and amenable for further interpretation than measurements commonly made with other assay systems, such as the phagokinetic track assay. In particular, measurements of this type are necessary for developing and evaluating mechanistic models of cell motility.

Application of the persistent random walk model allowed us to distinguish rigorously individual cells with different motile characteristics. With this approach qualitative comparisons between the structures of individual cell paths, which by themselves cannot separate differences in speed of movement from changes in turning behavior, can be placed in a quantitative framework with the parameters speed S and persistence time P. Because we fit experimental data using the full nonlinear relationship for the mathematical model (Eq. 1), instead of the linearized form used in some previous works (Dunn, 1983; Dow et al., 1987a), values for these parameters are independent of discretization rate (Farrell et al., 1990). The accuracy of this approach depends on sampling interval, tracking duration, and the migratory characteristics of cell type: sampling rate must be smaller than persistence time so that persistent behavior at short-time scales is not obscured, while the duration the cell is tracked must be several multiples of its persistence time to accurately observe the full turning behavior of the cell. Also, although the presence of immotile cells has been acknowledged in studies of neutrophil (Wilkinson et al., 1984), macrophage (Farrell et al., 1990), and microvessel endothelial cell migration (Stokes et al., 1991), to our knowledge our work is the first to positively and quantitatively discern immotile from motile tissue cells. The strict application of morphological criteria, such as the presence of a single well-defined lamellipod and uropod easily identifiable on motile white blood cells (Zigmond et al., 1981), is qualitative, rather than quantitative, for tissue cells observed under relatively low magnification.

The framework provided by the mathematical models of Alt (1980), Othmer et al. (1988), and Rivero et al. (1989) allows measurements of single-cell motility parameters to be interpreted in the context of cell population behavior (see Farrell et al., 1990). Our measurements of individual cell speed ($S\sim$ 10-20 micron/h) and persistence time ($P\sim$ 2-4 h) are similar to values previously determined for other tissue cells, including microvessel endothelial cells (Stokes et al., 1991). Consistent with this observation and Eq. 3, our estimates of the random motility coefficient μ for HSMCs on ECM-coated surfaces based on speeds and persistence times for motile cells are of the same order of magnitude ($\sim 10^{-9}$ cm^2/s) as direct measurements of this parameter for microvessel endothelial cells made using a linear under-agarose assay (Stokes et al., 1990). Glasgow et al. (1988) have suggested that neglecting immotile cells in calculating random motility coefficients from single-cell parameters may result in overestimates of μ. Alternatively, by interpreting immotile cells as merely resting cells and the parameter % motile cells as the fraction of time cells remain moving as opposed to resting, μ is simply reduced from the value calculated using Eq. 3 by the fraction of motile cells (Othmer et al., 1988). Which of these approaches is justified requires further examination of the behavior of apparently immotile cells.

Distributions of the model parameters provide additional quantitative insight into cell motile behavior not obvious from estimates of means and deviations. For instance, the excellent agreement between our experimental number distributions of persistence time and an exponential interarrival time distribution supports the proposition (Othmer et al., 1988) that the underlying stochastic process governing movement direction may result from a stationary Poisson process with intensity $\lambda_o = \overline{P}^{-1}$. However, even if the assumptions underlying Eq. 2 are appropriate for HSMCs (because the persistent random walk model can be derived from fundamentally different approaches, agreement between experimental data for HSMCs and Eq. 1 does not necessarily validate the underlying assumptions implicit in these developments), the measured values of λ_o are not only proportional to intrinsic Poisson intensities λ for random velocity changes but also are functions of the distribution of turning directions through the parameter ψ_d. Since human tissue cells move in curvilinear paths rather than linear segments connected by discrete turns, measurements of instantaneous cell re-orientation required for evaluating ψ_d are nontrivial. In contrast, by measuring the run lengths of individual bacteria, Phillips et al. (1991) recently have demonstrated both a normal speed distribution and an exponential number distribution of run lengths, or discrete displacements, for flagellated *E. coli* bacteria, a system in which independent measurement of ψ_d is possible (Berg and Brown, 1972).

Theoretical models have demonstrated that the relationship between surface composition and cell motility can be complex, depending on the relative influence of a number of biochemical and biophysical processes (DiMilla et al., 1991a). The variations in motile properties we observed among HSMCs on the three ECM substrata may result from the presence on HSMCs of differences in the number of cell surface adhesion receptors or the affinity of these receptors for these distinct protein ligands. Alternatively, coating a surface with the same soluble concentration of one of three proteins does not necessarily mean that the same bulk or active density of protein has adsorbed on each surface (DiMilla et al., 1992a). Using our experimental system we can now measure rigorously the effect of variations in the density of an adsorbed adhesive protein on cell speed and persistence time, and examine the predictions of mechanistic models for the role of cell-substratum adhesion

on migration (DiMilla et al., 1992b). In addition, with techniques from molecular biology, such as gene transfection, alterations in one or more of the molecular components involved in migration can be accomplished. Experimental measurements on these transfected cells can be used to test hypotheses concerning the underlying biochemical and biophysical properties responsible for cell movement (DiMilla et al., 1991b). Combined with these recent biological and modeling developments, the approach we have described here for measuring individual cell movement speed and persistence time should prove useful in future studies of the mechanistic factors responsible for the variations in motile behavior observed in different extracellular surroundings.

Acknowledgment

The authors would like to thank Dr. Stuart Williams of Thomas Jefferson University and Dr. Hynda Kleinman of the NIH for gifts of ECM proteins, Dr. Eliott Levine of the Wistar Institute for providing us with HSMCs, and Mildred Daise for help with cell culture. Brian Farrell and Martha Jones provided invaluable assistance in the development of the software required to analyze the motility of individual cells. We also thank Bret Phillips for many helpful discussions. This work was supported by a grant from the Whitaker Foundation to S. M. Albelda and NIH Grant GM-41476 to D. A. Lauffenburger. P. A. DiMilla also acknowledges financial support from a NSF Graduate Student Fellowship.

Notation

$\mathbf{C}$ = pixel-to-micron conversion factor (x-pixels/micron)
$d \cdot d$ = squared displacement, Eq. 4, micron^2
$\langle d \cdot d \rangle$ = mean-squared displacement, Eq. 5, micron^2
D^2_{max} = ratio of theoretical mean-squared displacement at t for $P = P_{min}$ to measured mean-squared displacement at $t = t_{max}/2$, Eq. 7
f = probability function for cell speed (Eq. 8) or persistence time (Eq. 9)
F_c = complement cumulative probability distribution, Eq. 10
% motile cells = fraction of cells observed, motile
n = dimensionality or current sampling interval number
N = number of sampling intervals cell tracked
P = persistence time, Eq. 2, h
$\overline{P}$ = mean persistence time, h
P_{min} = minimum allowed persistence time, min
S = root-mean-squared cell speed, micron/h
$\overline{S}$ = mean cell speed for motile cells, micron/h
t = time, min
Δt = cell centroid sampling time, min
t_d = time interval, min
t_{max} = total time cell tracked, min
t_{min} = minimum time interval used for fitting persistent random walk model to experimental data, min
x = x-axis coordinate for cell centroid, pixel
y = y-axis coordinate for cell centroid, pixel

Greek letters

λ = intensity of Poisson process for random velocity changes, min^{-1}
λ_o = inverse mean persistence time, h^{-1}
$\sigma_{d \cdot d}$ = standard deviation in mean squared displacement, Eq. 6, microns^2
σ_S = standard deviation in cell speed, micron/h
τ = discretization interval, min
μ = random motility coefficient, Eq. 3, cm^2/s
ψ_d = index of directional persistence

Literature Cited

Albelda, S. M., M. Daise, E. N. Levine, and C. A. Buck, "Identification and Characterization of Cell-substratum Adhesion Receptors on Cultured Human Endothelial Cells," *J. Clin. Invest.*, **83**, 1992 (1989).

Alt, W., "Biased Random Walk Models for Chemotaxis and Related Diffusion Approximations," *J. Math. Biol.*, **9**, 147 (1980).

Alt, W., "Correlation Analysis of Two-Dimensional Locomotion Paths," *Lecture Notes in Biomathematics: Biological Motion, Proc.*, p. 254, W. Alt and G. Hoffman, eds., Springer-Verlag (1990).

Berg, H., and D. A. Brown, "Chemotaxis in Escherichia Coli Analyzed by Three-Dimensional Tracking," *Nat.*, London, **239**, 500 (1972).

Bodin, Ph., S. Papin, C. Meyer, and P. Travo, "Study of Living Single Cells in Culture: Automated Recognition of Cell Behavior," *Lab. Invest.*, **59**, 137 (1988).

Boyden, W. V., "The Chemotactic Effect of Mixtures of Antibodies and Antigen and Polymorphonuclear Leukocytes," *J. Exp. Med.*, **115**, 453 (1962).

Clyman, R. I., D. C. Turner, and R. H. Kramer, "An $\alpha 1/\beta 1$-Like Integrin Receptor on Rat Aortic Smooth Muscle Cells Mediates Adhesion to Laminin and Collagen Types I and IV," *Arteriosclerosis*, **10**, 402 (1990).

Devore, J. L., *Probability and Statistics for Engineering and the Sciences*, Wadsworth (1991).

DiMilla, P. A., "Receptor-Mediated Tissue Cell Adhesion and Migration on Protein-Coated Surfaces," PhD Thesis, Univ. of Pennsylvania (1991).

DiMilla, P. A., K. Barbee, and D. A. Lauffenburger, "Mathematical Model for the Effects of Adhesion and Mechanics on Cell Migration Speeds," *Biophys. J.*, **60**, 15 (1991a).

DiMilla, P. A., J. A. Quinn, S. M. Albelda, and D. A. Lauffenburger, "Receptor/Ligand-Mediated Mechanisms for Cell Migration on Protein-Coated Surfaces," *Annals Biomed. Eng.*, **19**, 596 (1991b).

DiMilla, P. A., S. M. Albelda, and J. A. Quinn, "Adsorption and Elution of Extracellular Matrix Proteins on Nontissue Culture Polystyrene Petri Dishes," *J. Coll. Inter. Sci.*, accepted (1992a).

DiMilla, P. A., J. A. Stone, S. M. Albelda, D. A. Lauffenberger, and J. A. Quinn, "An Optimal Cell-Substratum Adhesiveness Exists for Smooth Muscle Cell Migration on Type IV Collagen and Fibronectin," *J. Cell. Biol.*, in preparation (1992b).

Dow, J. A. T., P. Clark, P. Connolly, A. S. G. Curtis, and C. D. W. Wilkinson, "Novel Methods for the Guidance and Monitoring of Single Cells and Simple Networks in Culture," *J. Cell Sci.* [*Suppl.*], **8**, 55 (1987a).

Dow, J. A. T., J. M. Lackie, and K. V. Crocket, "A Simple Microcomputer-Based System for Real-Time Analysis of Cell Behavior," *J. Cell Sci.*, **87**, 171 (1987b).

Dunn, G. A., "Characterizing a Kinesis Response: Time-Averaged Measures of Cell Speed and Directional Persistence," *Agents and Actions* [*Suppl.*], **12**, 14 (1983).

Farrell, B. E., R. P. Daniele, and D. A. Lauffenburger, "Quantitative Relationships between Single-Cell and Cell-Population Model Parameters for Chemosensory Migration Responses of Alveolar Macrophages to C5a," *Cell Motility and Cytoskel.*, **16**, 279 (1990).

Gail, M. H., and C. W. Boone, "The Locomotion of Mouse Fibroblasts in Tissue Culture," *Biophys. J.*, **10**, 980 (1970).

Glasgow, J. E., B. E. Farrell, E. S. Fisher, D. A. Lauffenburger, and R. P. Daniele, "The Motile Response of Alveolar Macrophages: an Experimental Study Using Single-Cell and Cell Population Approaches," *Amer. Rev. Resp. Dis.*, **139**, 320 (1989).

Goodman, S. L., G. Risse, and K. von der Mark, "The E8 Subfragment of Laminin Promotes Locomotion of Myoblasts Over Extracellular Matrix," *J. Cell. Biol.*, **109**, 799 (1989).

Keller, E. F., and L. A. Segel, "Model for Chemotaxis," *J. Theor. Biol.*, **30**, 225 (1971).

Lackie, J. M., *Cell Movement and Cell Behavior*, Allen and Unwin (1986).

Lauffenburger, D., "Measurement of Phenomenological Parameters for Leukocyte Motility and Chemotaxis," *Agents and Actions* [*Suppl.*], **12**, 34 (1983).

Lewis, L., and G. Albrecht-Buehler, "Distribution of Multiple Centrospheres Determines Migration of BHK Syncitia," *Cell. Motility and Cytoskel.*, **7**, 282 (1987).

Majack, R. A., and A. W. Clowes, "Inhibition of Vascular Smooth

Muscle Cell Migration by Heparin-like Glycosaminoglycans," *J. Cell. Physiol.*, **118**, 253 (1984).
Othmer, H. G., S. R. Dunbar, and W. Alt, "Models of Dispersion in Biological Systems," *J. Math. Biol.*, **26**, 263 (1988).
Parkhurst, M. R., and W. M. Saltzman, "Quantification of Human Neutrophil Motility in Three-Dimensional Collagen Gels: Effect of Collagen Concentration," *Biophys. J.*, **61**, 306 (1992).
Phillips, B. R., J. A. Quinn, and H. Goldfine, "Transport Behavior of Motile Bacteria: Measurement and Prediction of Motility Parameters," AIChE Meeting, Los Angeles (1991).
Pratt, B. M., A. S. Harris, J. S. Morrow, and J. A. Madri, "Mechanisms of Cytoskeletal Regulation: Modulation of Aortic Endothelial Cell Spectrin by the Extracellular Matrix," *Amer. J. Pathol.*, **117**, 349 (1984).
Press, W. H., B. P. Flannery, S. A. Teukolsky, and W. T. Vetterling, *Numerical Recipes: the Art of Scientific Computing*, Cambridge University Press (1986).
Rivero, M. A., R. T. Tranquillo, H. M. Buettner, and D. A. Lauffenburger, "Transport Models for Chemotactic Cell Populations Based on Individual Cell Behavior," *Chem. Eng. Sci.*, **44**, 2881 (1989).
Ross, R., "The Pathogenesis of Atherosclerosis: an Update," *New Eng. J. Med.*, **314**, 488 (1986).
Sato, Y., R. Hamanaka, J. Ono, M. Kuwano, D. B. Rifkin, and R. Takaki, "The Stimulatory Effect of PDGF on Vascular Smooth Muscle Cell Migration Is Mediated by the Induction of Endogenous Basic FGF," *Biochem. Biophys. Res. Comm.*, **174**, 1260 (1991).
Singer, S., and A. Kupfer, "The Directed Migration of Eukaryotic Cells," *Ann. Rev. Cell. Biol.*, **2**, 337 (1986).
Soll, D. R., E. Voss, B. Varnum-Finney, and D. Wessels, "Dynamic Morphology System: a Method of Quantitating Changes in Shape, Pseudopod Formation, and Motion in Normal and Mutant Amoebae of Dictyostelium discoideum," *J. Cell. Biochem.*, **37**, 177 (1988).
Stokes, C. L., M. A. Rupnick, S. K. Williams, and D. A. Lauffenburger, "Analysis of the Roles of Endothelial Cell Motility and Chemotaxis in Angiogenesis," *Lab. Invest.*, **63**, 657 (1990).
Stokes, C. L., D. A. Lauffenburger, and S. K. Williams, "Migration of Individual Microvessel Endothelial Cells: Stochastic Model and Parameter Measurement," *J. Cell Sci.*, **99**, 419 (1991).
Straus, A. H., W. G. Carter, E. A. Wayner, and S.-I. Hakomori, "Mechanism of Fibronectin-Mediated Cell Migration: Dependence or Independence of Cell Migration Susceptibility on RGDS-directed Receptor (Integrin)," *Exp. Cell Res.*, **183**, 126 (1989).
Tan, E. M. L., G. R. Dodge, T. Sorger, I. Kovalszky, G. A. Unger, L. Yang, E. M. Levine, and R. V. Iozzo, "Modulation of Extracellular Matrix Gene Expression by Heparin and Endothelial Cell Growth Factor in Human Smooth Muscle Cells," *Lab. Invest.*, **64**, 474 (1991).
Trinkaus, J. P., *Cells Into Organs: the Forces that Shape the Embryo*, Prentice-Hall, Englewood Cliffs, NJ (1984).
Wilkinson, P. C., J. M. Lackie, J. V. Forrester, and G. A. Dunn, "Chemokinetic Accumulation of Human Neutrophils on Immune-Complex-Coated Substrata: Analysis at a Boundary," *J. Cell Biol.*, **99**, 1761 (1984).
Zigmond, S. H., H. I. Levitsky, and B. J. Kreel, "Cell Polarity: An Examination of Its Behavioral Expression and Its Consequences for Polymorphonuclear Leukocyte Chemotaxis," *J. Cell. Biol.*, **89**, 585 (1981).

Manuscript received Nov. 22, 1991, and revision received Mar. 30, 1992.